Modeling and simulation of low pressure oil-hydraulic pipeline transients

Dan Jiang[1, 3], Songjing Li[1*], Kevin A. Edge[2*] and Wen Zeng[1]

[1]Department of Fluid Control and Automation, Harbin Institute of Technology, Harbin, China

[2]Centre for Power Transmission and Motion Control, University of Bath, Bath, UK

[3]School of Mechatronics Engineering, University of Electronic Science and Technology of China, Chengdu, China

Abstract: In order to predict more accurately the pressure transients accompanying air release and vaporous cavitation inside oil-hydraulic low pressure pipelines, a new method using genetic algorithms (GAs) for parameter identification is described. A mathematical model for pressure and flow transients is presented in which models of vaporous cavitation and dynamic air release and re-solution are incorporated. This model enables the prediction of both the vaporous cavitation and the air bubble volumes in the pipeline during the transients following a sudden cut-off of the flow. The accurate prediction of behavior largely depends on three generally unknown parameters required by the model, namely: the initial air bubble volume in the oil, and the air release and re-solution time constants. Through the use of the GAs, these parameters can be identified. Predicted results and experimental data show close correspondence.

Keywords: pressure transients, parameter identification, genetic algorithms, cavitation, air release

*Corresponding authors:

Songjing Li, Department of Fluid Control and Automation, Harbin Institute of Technology, Harbin, China. Email:lisongjing@hit.edu.cn

Kevin A. Edge, Center for Power Transmission and Motion Control, University of Bath, Bath, UK. Email: enskae@bath.ac.uk

1 INTRODUCTION

Pressure transients accompanying air release and vaporous cavitation in hydraulic low-pressure pipelines, such as in the suction line of a hydraulic pump or the return line of a hydraulic system, are generally undesirable as they can lead to performance deterioration and damage. The presence of air and vapour cavities also influences pressure transient behaviour in hydraulic pipelines. For an accurate assessment of performance and as an aid to the design of hydraulic pumps and systems, it is of great importance to be able to predict, accurately, the pressure transients accompanying air release and cavitation.

The modeling and simulation of air release and cavitation in pipelines has been studied by a number of authors [e.g. **1**-**4**] but still presents a significant challenge. The lack of appropriate parametric data adds to the difficulty.

In recent years, the research in this area has focused on developing models for the prediction of pressure transients occurring in high pressure pipelines under non-cavitation conditions [e.g. **5, 6]**. However, these models are unsuited for the prediction of behavior of low pressure pipelines where cavitation and air release is occurring. For most mineral oil based hydraulic systems, the oil contains dissolved air. More generally, the types of liquid being conveyed in pipelines can contain other types of dissolved gas - CO_2 for example. In order to take account of gas release in the modeling of cavitation in liquid piping systems, Kranenburg **[7]** described the rate of gas release and re-solution as a function of gas bubble radius, pressure and relative velocity of gas bubbles in the liquid phase. However, the determination of the gas bubble radius and the relative velocity is based solely on judgment or an empirical formula. Hence this approach is unlikely to be appropriate as a means of predicting transient behavior. Wylie and Streeter **[8]** made assumptions that the gas release process follows Henry’s law, but no attempt was made to explain the influence of release rate on pressure transients in hydraulic pipelines.

Wiggert **[9]** analyzed the effect of gas release on pressure transients and identified that the greatest uncertainty in the models was the rate of gas release. Baasiri [**10]** investigated both experimentally and numerically air release during column separation and attempted to develop empirical equations for the rate of air release and re-solution. Kojima **[11]** undertook experimental studies using a spool-type directional control valve in a housing made of transparent acrylic resin which was mounted at the end of a piping system. A high-speed camera was employed to record the growth and collapse of air bubbles following sudden closure of the valve. A "gas-nonbubbly flow" model considering the effects of released gas inside the separated cavity and of an unsteady pipe friction was developed for the prediction of oil-hydraulic pipeline pressure transients. Reasonably good accuracy was achieved, but nonetheless there were some discrepancies between simulation and experimental results. Akagawa [**12**] conducted various analytical methods and experiments including experiments for a two-phase air-water flow and a one-component two-phase flow, theoretical analysis of the magnitude of pressure rises and linearization analysis of pressure transients. Zielke [**13**] studied the characteristic time scale of the transients and the gas release in pipe flow. A common problem with the majority of existing models is that, whilst air-release is generally taken to follow first-order dynamics [**14**], there is no agreement yet on what time constants are appropriate to model air release and re-solution and what might be a representative value for the initial air bubble volume.

In order to simulate numerically the pressure transients accompanying vaporous cavitation and air release/re-solution in low pressure pipelines, a model is presented here which attempts to capture the key features but without being unduly complex. Parameter identification is carried out by means of genetic algorithms (GAs) whose objective function is the sum of the least-square errors between experimental data and simulation results. The aim is to perform a global search to obtain optimal parameters suitable for pressure transient modeling.

2 MATHEMATICAL MODELS AND SIMULATION METHOD

2.1 Basic equations under non-cavitating conditions

The principal equations for the simulation of pressure transients inside a pipeline under non-cavitating conditions are well-established. In this paper, a time- and spatial-discretisation method is adopted for their solution with amendments to account for behavior when the pressure within any discrete pipeline element falls below the saturated vapor pressure.

The continuity equation, as an expression of mass conservation, can be described as:

$$\frac{1}{c_0^{\,2}}\frac{\partial p}{\partial t}+\frac{\rho}{\pi r_0^{\,2}}\frac{\partial q}{\partial x}=0 \tag{1}$$

The motion equation, as an expression of momentum conservation, can be described as:

$$\frac{\rho}{\pi r_0^{\,2}}\frac{\partial q}{\partial t}+\frac{\partial p}{\partial x}+F(q)+\rho g\sin\theta_0=0 \tag{2}$$

In the continuity equation (1), the acoustic velocity in the oil c_0 can be written as:

$$c_0=\sqrt{\rho/B_{eff}} \tag{3}$$

where, ρ is the density and B_{eff} is the effective bulk modulus of mixture. In the motion equation (2), the frictional force due to the fluid viscosity $F(q)$ can be described as:

$$F(q)=F_0+\frac{1}{2}\sum_{i=1}^{4}Y_i \tag{4}$$

where, the first item F_0 is the steady state friction and the second item is the frequency-dependent unsteady friction. Y_i can be calculated from:

$$\begin{cases}\dfrac{\partial Y_i}{\partial t}=-\dfrac{n_i\mu}{\rho r_0^{\,2}}Y_i+m_i\dfrac{\partial F_0}{\partial t} & (i=1,\ 2,\ 3,\ 4)\\ Y_i(0)=0\end{cases} \tag{5}$$

The constants n_i and m_i are given by Taylor [**15**].

The specific case considered here is a length of straight pipe of uniform cross-section. In order to

solve the two partial differential equations in terms of pressure and flow rate, the pipeline is divided into n elements of equal length. The scheme has been implemented using the Matlab/Simulink platform. The variables of flow rate and pressure are created as vectors. For the n elements, the vectors of flow rate and pressure inside the pipeline are:

$$\boldsymbol{q} = (q_1 \quad q_2 \quad \ldots \quad q_n)^{\mathrm{T}},$$

$$\boldsymbol{p} = (p_1 \quad p_2 \quad \ldots \quad p_n)^{\mathrm{T}}.$$

The partial derivative terms in time domain, $\partial/\partial t$, can be readily calculated using the integral block in Simulink.

For the solution of the partial derivatives terms in the spatial domain, $\partial/\partial x$, an approach has been developed which makes use of the Simulink Selector Block. Taking the boundary condition q_0 (in this case q_0 =0) and the first n–1 number of elements together, the Selector Block is used to re-order specified elements of the vector. For the case of the flow rate, a new flow rate vector $\boldsymbol{q}'$ is formed, such that,

$$\boldsymbol{q}' = (q_0 \quad q_1 \quad \ldots \quad q_{n-1})^{\mathrm{T}}$$

Hence $\partial\boldsymbol{q}/\partial x$ can be described as:

$$\frac{\partial \boldsymbol{q}}{\partial x} \approx \frac{\boldsymbol{q} - \boldsymbol{q}'}{\Delta x} \tag{6}$$

For the pressure vector, the Selector Block is used to create a new pressure vector $\boldsymbol{p}'$, thus

$$\boldsymbol{p}' = (p_2 \quad \ldots \quad p_n \quad p_0)^{\mathrm{T}}$$

where p_0 is the boundary condition.

So that $\partial\boldsymbol{p}/\partial x$ can be described as:

$$\frac{\partial \boldsymbol{p}}{\partial x} \approx \frac{\boldsymbol{p}' - \boldsymbol{p}}{\Delta x} \tag{7}$$

More technical details about the discretion of the equation can be seen in Ref. [**6**].

2.2 Air release and re-solution

Generally, it is accepted that the volume of free air can be treated as a fixed volume during very rapid and short duration transients [**16**]. Nevertheless, Ref. [**14**] introduced that air-release process was taken to follow the first-order dynamics. Therefore, the dynamic volume change of air bubbles in the pipeline can be considered during the transients.

When the pressure falls below the equilibrium condition for the air dissolved in the oil, air bubbles form. This is not an instantaneous effect, and is dependent on a number of factors including the type of liquid, its temperature, and the degree of "agitation" present. The presence of air in the form of bubbles changes the effective bulk modulus of hydraulic oil significantly. This has a consequent effect on the acoustic velocity and damping of pressure transients. Even very small quantities of air in the form of bubbles can have a significant effect on system behavior.

Henry's law states that in the case of equilibrium (when the liquid can neither release nor dissolve more air), the volume of dissolved air in the liquid is proportional to the absolute pressure p_e:

$$v_e = S\frac{p_e}{p0}V \tag{8}$$

where S is the solubility constant of air. For a mineral oil hydraulic system, the oil contains around 9-10% of dissolved air at atmospheric pressure $p0$ at 20 ºC. V is the volume of hydraulic oil with the presence of vapor cavities and air bubbles.

The instantaneous air bubble volume in the oil V_{air} is expressed, in aggregate, as an initial bubble volume V_{iniair} plus the difference between volume of air dissolved in the oil at the initial condition v_e and the volume of air v dissolved at time t. It is assumed that initially the dissolved oil is in equilibrium.

$$V_{air} = V_{iniair} + v_e - v \tag{9}$$

The rate of air release/re-solution can be calculated from:

$$\dot{v} = \frac{v_\infty - v}{\tau} \tag{10}$$

When the pressure falls below the equilibrium condition, the air is released and τ is defined as the air release time constant τ_r; when the pressure recovers, the air is resolved and τ is defined as the air re-solution time constant τ_s. v_∞ is the volume of air dissolved in the oil at pressure p, which can be written as:

$$v_\infty = v_e \frac{p}{p_e} \tag{11}$$

If there is no air bubbles inside the oil, the acoustic velocity c_0 is constant because the effective bulk modulus B_{eff} is equal to the bulk modulus of liquid B_{liquid}. But if there are air bubbles presented in the oil, the effective bulk modulus of the air and oil mixture can be described as:

$$B_{eff} = \frac{B_{air} B_{liquid}}{(V_{air}/V)(B_{liquid} - B_{air}) + B_{air}} \tag{12}$$

where, B_{air} and B_{liquid} are the bulk modulus of air and liquid, respectively.

2.3 Continuity equation under vaporous cavitating conditions

When the pressure falls to the vapor pressure of the liquid, vaporous cavitation occurs. This is a complex thermodynamic phenomenon which has been addressed in detail by Chochia et al [**17**]. However, previous studies on piston pumps [**18**, **19**] have demonstrated that a relatively simple column separation model can capture the key aspects of cavitation. That approach is adopted here. In accordance with the flow continuity principle, under column separation the volume of cavitation V_{cav} can be presented as:

$$\frac{dV_{cav}}{dt} = q_{out} - q_{in} \tag{13}$$

where, q_{out} and q_{in} are the outflow rate and inflow rate of an element in the pipe, respectively. Under vaporous cavitating conditions, the pressure in the element is assumed to be the vaporous pressure.

3 SIMULATION RESULTS

A study has been conducted to predict the fluid transients in a system comprised of a horizontally-mounted straight length of pipe, of constant cross-sectional area, in which fluid is initially flowing at a constant velocity. One end of the pipe is taken to be connected to a reservoir at atmospheric pressure and a shut-off valve is mounted the opposite end. The initial aim was to predict behaviour following instantaneous closure of the valve. System parameters are given in Table 1. The results presented here correspond to a 20 element discretisation which was previously found to be appropriate; the sensitivity of the predictions to the number of elements selected has been considered elsewhere [**20**]. The first element is that which is adjacent to the valve and the last element is adjacent to the reservoir. The simulation period was set to 0.11s and variable-step solver, ode23s, was used for numerical integration.

Table 1 Parameters in the simulation

For any hydraulic system, it is difficult to specify the distribution of air bubbles in the oil and their initial volume. In order to investigate the influence of air bubbles at the initial conditions, simulation runs were undertaken assuming initial air bubble volumes of 0.1%, 1%, and 3% of the element volume with a uniform distribution throughout the pipeline. As an illustration, the pressure transient in the element corresponding to the position of the first transducer (used in the experimental work, as described later), following sudden valve closure, is shown in Fig. 1. In this case, the time constants τ for the re-solution and release of air were chosen to be 10s and 5s respectively. As shown in Ref [**14**], the air release process is usually faster than the air re-solution process for mineral oils. Comparison of the three graphs shows that the initial volume of air bubbles present in the system is predicted to have a significant effect on transient behaviors, and hence is an important parameter.

Fig. 1 Pressure pulsations with different initial volume of air bubbles

In order to investigate the influence of time constants, predictions of pressure transients were also carried out using different air release and re-solution time constants, as well as solubility constant *S*, as shown in Table 2. These correspond to the values presented by Schweitzer and Szebehely **[14]**. The initial volume of air bubbles was assumed to be 0.5% of the element volume, again with a uniform distribution throughout the pipeline. Figure 2 shows, for the case of the fourth element, very different pressure histories for the three sets of parameters in Table 2. This was also found to be the case at other locations in the pipeline. With the larger time constants, the cavitation is almost entirely vaporous, because the quantity of air that can be released in the time available is very small. In order to investigate the sensitivity of the pressure transient prediction to just the air release time constant, three sets of simulations were undertaken using the data in Table 3. Figure 3 illustrates the corresponding pressure predictions in the fourth element. It is clear that the greater difference lies between the predicted transients for air release time constants of 0.5s and 5s as opposed to time constants of 5s and 50s. Further simulations revealed that the sensitivity increased significantly with time constants of less than 1s.

Table 2 Parameters of air releasing and resolving time constants and solubility constant

Fig. 2 Pressure transients for the parameters in Table 2

Table 3 Parameters of air release time constant

Fig. 3 Pressure transients for the parameters in Table 3

From these preliminary studies, it can be observed that the initial volume of air bubbles, and the air

release and re-solution time constants can have a significant effect on pressure transients. In order to achieve more accurate simulations, it is vital that correct parameter identification is made to establish typical values for these parameters in real systems.

4 OPTIMIZED RESULTS

Parameter identification was carried out by using the experimental data to select reasonable parameter values. Applying the proposed GAs, experimental data were used to calculate the fitness function. These experimental data were obtained by measuring the pressure transients in a horizontal hydraulic pipeline following a rapid closure at one end. Figure 4 shows the schematic layout of test rig. A reservoir at one end of the pipeline provided a constant upstream pressure as one boundary condition. The pipeline was connected to the suction port of a small gear pump (4.8 ml/rev) driven by a variable speed electric motor. Previous studies on other, similar, test facilities had shown that it is very difficult to use a valve to achieve very rapid shut-off of flow in a pipeline ('rapid' being relative to the dynamics of the induced pressure transients). Electrically-actuated valves rarely have sufficient bandwidth to meet the requirements and it is very difficult to achieve consistent results with manually-operated valves. For the investigation report here, a novel approach was adopted, as proposed by Mancó (see Acknowledgements). The pump was started with its speed set to achieve a particular flow rate in the pipeline. To achieve very rapid shut-off of the flow in pipeline, a steel ball was released from the reservoir. The ball, which had a diameter of 10 mm, was carried along by the flow in the pipeline until it hit a seat immediately upstream the suction port of the pump. Strong magnets were mounted in close proximity to the seat to assist in preventing the ball from bouncing. This technique was found to work well for low to medium flow rates (less than 2×10^{-4} m^3/s). However, at higher flow rates, the pressure differential required to accelerate the ball was found to create air bubbles immediately behind it, as it travelled along the pipeline. Also, the ball was found to bounce from its seat when higher flow rates

were studied. The work reported here is only concerned with studies at low to medium flow rates. In order to observe visually the nature of the growth and collapse of vapour cavities and air bubbles during the transients, a 129 mm long transparent viewing tube, with the same internal bore as the pipe, was mounted at the ball seat. Behaviour was recorded using a high speed video camera running at 500 frames per second.

Two piezoelectric pressure transducers, fitted to the pipe at different locations, were used to record pressure transients. These signals were sampled at 10 kHz. Hence two sets of experimental data were obtained. One is for model parameter identification by GAs, the other for validating efficiency of pressure transient models with optimized parameters. In procedure of GAs, experimental data were obtained from the pressure transducer closest to the valve seat.

Fig. 4 Principle scheme for the experiments

For the optimization procedure, the parameters were encoded in binary form and the GAs were set up for a population of chromosomes made up of 3 genes, comprising the initial air bubble volume, air release time constant and air re-solution time constant. The algorithm parameters are summarized in Table 4 and the results of the parameter identification (for the case of a flow rate of 8.7×10^{-5} m^3/s) are reported in Table 5.

Table 4 Genetic algorithm parameters

Table 5 Results of parameter identification

The adoption of these identified parameters in the pressure transient mathematical models led to the pressure results in the element, where the first transducer is placed, is illustrated in Fig. 5. In the same

figure, the simulation results of mathematical models using the No. 1 set of parameters in Table 3 are also reported. Clearly the simulation using the identified parameters provides better accuracy, especially in terms of the magnitude of the first pressure peak and the timing of the subsequent peaks.

Fig.5 Comparison of simulation and experimental pressure transients at the first transducer

In the numerical simulation results, at the beginning of each pressure surge, high frequency oscillations can be seen immediately on flow stoppage. It is due to the numerical method of the discretisation which has a relationship with the discreting element number of the pipeline. With the increasing of element number, pressure oscillations at the top of each pulsation will vanish.

The experimental pressure data from the second transducer is compared with the corresponding simulation results of the optimal model in Fig. 6. As can be seen, there is a good agreement between the two curves. Comparison of the results demonstrates that the optimization using GAs is capable of providing a good estimation of unknown parameters in the model. It is interesting to note that in the work of Pettersson et al [**18**], on the simulation of cavitation and air release in a fluid power piston pump, the authors report excellent agreement between predictions and experiment when using a time constant of 0.5s for both air release and re-solution. This is significantly smaller than values found in the studies report in this paper. A possible explanation is the much greater degree of "agitation" of the fluid that takes place in a pump, when compared to the conditions in a pipeline.

Fig.6 Comparison of simulation and experimental pressure transients at the position of the second transducer

For a lower flow rate, the comparisons between simulation and experimental pressure transients are shown in Fig.7 a) and b), respectively (for the case of a flow rate of 4.3×10^{-5} m^3/s). In the simulation, it is assumed that initial air bubble volumes are associated with the type of liquid and its temperature.

Therefore, both at the lower initial flow rate and at the higher initial flow rate, the same values of identified parameters for the initial volumes of air bubble are adopted. It can be seen that the mathematical model with the identified parameters is also reasonable for the prediction under different flow rate conditions. Compared with the results above at the medium flow rate (8.7×10^{-5} m^3/s), the magnitude of the pressure peaks and the duration between them are decreased at the lower flow rate.

a) At the position of the first transducer

b) At the position of the second transducer

Fig.7 Comparison of simulation and experimental pressure transients at the lower flow rate

5 VERIFICATION OF IDENTIFIED RESULTS

In order to assess the nature of the air release and vaporous cavitation predicted by the model, consider the pressure transient in the first element shown in Fig. 8 (for the case of a flow rate of 8.7×10^{-5} m^3/s). This is similar to the behaviour in the element where the first transducer is placed, but the first pressure peak appears earlier. The corresponding cavitation and air bubble volumes are shown in Fig.9. The maximum size of the vaporous cavity is 5.5×10^{-7} m^3 and exists for around 40 ms. The air bubble volume is smaller than cavitation volume, but it remains present throughout. The air bubble volume increases overall because the time constant for air release is smaller than for re-solution.

Fig. 8 Simulation result for the pressure transients in the first element

Fig.9 Predicted cavitation and air bubble volumes in the first element

Figure 10 illustrates the growth and collapse of the cavities in the viewing tube recorded by the high speed video camera. The eight photographs correspond to the points labelled A to H in Fig. 8. Once the ball hits the seat (B), a pressure pulse is created which then propagates from the ball to the reservoir. The pressure then falls to the vapour pressure, with cavities growing quickly reaching their maximum size at the ball face, as shown in (C). From the photographs, it is not possible to differentiate between vapour and air, but from Fig. 9 it is notable that at its peak, the vapour volume is dominant, being around 50 times larger than the air volume. From the photograph in Fig. 10C, the cavitation volume can be roughly estimated to be the same as the ball volume, which is $5.23\times10^{-7}m^3$. This agrees well with the maximum volume predicted in Fig. 9. The pressure rises again when the pressure pulse travels back toward the ball seat, and the vapour cavity collapses and disappears from photograph (D). The volume of air bubbles predicted to remain at this condition is too small to be visible in the photograph. When the pressure falls again, cavity growth can again be seen (E) but is much smaller than at C. Once again the cavity collapses at the arrival of the third pressure peak (F). At last, the cavity and air bubbles experience the third time of growth and collapse (G and H). The simulation results for the pressure transients, wave propagation times, and, in broad terms, the cavity volume, correspond well with the photographic images. Overall, the low pressure transient model with optimal parameters provides an effective prediction of observed behaviour. The video of the cavitation behaviour during the pipeline transients recorded by the high speed video camera in the first element is shown in video 1.

Fig.10 Record of cavitation behaviour in the first element

Video 1 Cavitation behaviour in the first element

6 CONCLUSIONS

A study has been undertaken to model the pipeline transients and to identify the values of key parameters for use in the modeling of pressure transients in low pressure oil-hydraulic pipeline. The following conclusions are drawn:

1. The low pressure oil-hydraulic pipeline transient models are given by considering the behavior of gas bubbles and cavitation in this paper.
2. The comparison of simulation results and experimental data shows that the low pressure oil-hydraulic pipeline transient models can capture the key feature of the fluid transients.
3. A GA-based parameter identification scheme is an effective means to obtain the reasonable values of parameters in the low pressure oil-hydraulic pipeline transient models.
4. The identified parameters may only be applicable for the specific conditions of the experiment in this paper. Further work needs to be undertaken to find out the extent to which these values can be applied under other test conditions.

ACKNOWLEDGEMENT

The authors would like to thank sincerely Dr. Salvatore Mancó of Politecnico di Torino, Italy, for providing the hydraulic pump and electric drive used in the test rig at University of Bath, and also for introducing the authors to the use of a steel ball as the means to achieve rapid shut-off of the flow.

REFERENCES

1 **Shu, J.**, **Burrows, C. R.** and **Edge, K. A.** Pressure pulsation in reciprocating pump piping systems Part1: modelling, *Proc. Inst. Mech. Engrs., Part I*, 1997, **211**, 229-237.

2 **Shu, J..** Modeling vaporous cavitation on fluid transient. *International Journal of Pressure Vessels and Piping*, 2003, **80**, 187-195.

3 **Bergant, A.** and **Simpson, R. S.** Pipeline column separation flow regimes. *Journal of Hydraulic Engineering*, 1999, **125**(11), 835-848.

4 **Lee, I. Y., Kitagawa, A.** and **Takenaka, T.** On the transient behavior of oil flow under negative pressure, *Bull. JSME*, 1985, **28**, 1097–1104.

5 **Shu, J.-J.** A finite element model and electronic analogue of pipeline pressure transients with frequency-dependent friction. *Journal of Fluids Engineering*, 2003, **25**(1), 194-198.

6 **Li, S., Edge, K. A.** and **Bao, W.** Simulation of hydraulic pipeline pressure transient using Matlab Simulink, In *Proceedings of the Sixth International Conference on Fluid Power Transmission and Control*, 2005, 468-471.

7 **Kranenburg, C.** Gas release during transient cavitation in pipes, *Hydro Div*, ASCE, 1974, **10**, 11-15.

8 **Wylie, E. B., Streeter, V. L.** Fluid transients, McGraw-Hill, 1978.

9 **Wiggert, D. C.** and **Sundquist, M. J.** The effect of gaseous cavitation on fluid transients, *Journal of Fluids Engineering*, 1979, **101**, 79-86.

10 **Baasiri, M.** and **Tullis J. P.** Air release during column separation. *Journal of Fluids Engineering*, 1983, **3**, 113-117.

11 **Kojima, E., Shinada, M.** and **Shindo, K.** Fluid transient phenomena accompanied with column separation in fluid power pipeline. *Bull. JSME*, 1984, **27**(233): 2421-2429.

12 **Akagawa, K.,** and **Fujii, T.** Development of research on waterhammer phenomena in two-phase flow: progress in our research unit at kobe university. *ASME-JSME Thermal Engineering Joint Con*., Honolulu, 1987, 333-349.

13 **Zielke, W., Perko, H.D.,** and **Keller, A**. Gas release in transient pipe flow. *Proc. 6th Int. Conf. Pressure Surges BHRA*, Cambridge, England, 1989, 3-13

14 **Schweitzer, P. H.** and **Szebehely, V. G.** Gas evolution in liquids and cavitation. *Journal of Applied Physics*, 1950, **21**(12), 1218-1224.

15 **Taylor, S. E. M., Johnston, D. N., Longmore, D. K.** Modeling of transient flow in hydraulic pipelines. *Proc. Inst. Mech. Engrs., Part I*, 1997, **211,** 447-456.

16 **Bergant, A., Simpson, A. R.,** and **Tijsseling, A. S.** Water hammer with column separation: A historical review. *Journal of Fluids and Structures*, 2006, 22, 135-171

17 **Chochia**, **G. A., Tilley, D.G.** and **Nguyen-Schaefer, H.** Numerical and experimental investigations on a shock wave related cavitation flow. *Proc. Inst. Mech. Engrs., Part I*, 2001, **215**, 71-91.

18 **Pettersson, M., Weddfelt, K.** and **Palmberg, J. O.** Modelling and measurement of cavitation and air release in a fluid power piston pump. *Third Scandinavain Conf. on Fluid Power, Linköping, Sweden, May 25-26, 1993*

19 **Harris, R.M., Edge, K.A.** and **Tillley, D.G.** The suction dynamics of positive displacement axial piston pumps. *Journal of Dynamic Systems, Measurement and Control*, 1994, **116**(2), 281-287.

20 **Jiang D.** and **Li S.** Simulation of hydraulic pipeline pressure transients accompanying cavitation and gas bubbles using Matlab/Simulink. *2006 ASME Joint U.S.-European Fluids Engineering Summer Meeting*, 2006, 657-665

Notation

B_{air} bulk modulus of air (Pa)

B_{eff} effective bulk modulus (Pa)

B_{liquid} bulk modulus of liquid (Pa)

c_0 acoustic velocity in hydraulic oil (m/s)

$F(q)$ frictional force arising from fluid viscous effects (N)

F_0 steady state friction (N)

g acceleration due to gravity (m/s^2)

p pressure at some point along the pipeline (Pa)

p_e equilibrium pressure (Pa)

p_0 pressure at reservoir (Pa)

$p0$ atmospheric pressure (Pa)

q flow rate at some point along the pipeline (m^3/s)

q_{in} inflow rate (m^3/s)

q_{out} outflow rate (m^3/s)

r_0 internal radius of pipeline (m)

S solubility constant

t time variable (s)

V volume of hydraulic oil with vapor cavities and air bubbles present (m^3)

V_{air} volume of air bubbles (m^3)

V_{cav} volume of vaporous cavities (m^3)

V_{iniair} initial volume of air bubbles (m^3)

x space variable (m)

Y_i frequency dependent unsteady friction (N)

θ_0 angle of hydraulic pipeline inclined to the horizontal (rad)

μ dynamic viscosity of hydraulic oil (Pa • s)

ρ density of air and liquid mixture in the pipeline (kg/m^3)

τ time constant(s)

τ_r time constant for air release(s)

τ_s time constant for air re-solution (s)

v volume of air dissolved inside the oil (m3)

v_e volume of air dissolved in the oil at pressure pe under equilibrium conditions (m3)

v_∞ volume of air dissolved in the oil at pressure p under equilibrium conditions (m3)

Table 1 Parameters in the simulation

Parameters	Values
Bulk modulus of hydraulic oil	16000 bar
Kinetic viscosity of hydraulic oil	44 mm^2/s
Density of hydraulic oil	875 kg/m^3
Head in reservoir	0.3 m
Initial flow rate	8.7×10^{-5} m^3/s
Pipeline internal diameter	0.0102 m
Length of test pipeline	3.856 m
Maximum time step	0.0001 s

Table 2 Parameters of air releasing and resolving time constants and solubility constant

No.	Air release time const. (s)	Air re-solution time const. (s)	Solubility const. (%)
1	0.43	4.44	11.98
2	5.13	8.86	10.72
3	65	557	8.15

Table 3 Parameters of air release time constant

No.	Air release time const. (s)	Air re-solution time const. (s)	Solubility const. (%)
1	0.5	100	10
2	5	100	10
3	50	100	10

Table 4 Genetic algorithm parameters

Parameters	Values
Number of generations	30
Number of chromosomes	20
Selection method	roulette
Crossover probability	0.4
Mutation probability	0.005

Table 5 Results of parameter identification

Identified parameters	Values
Initial volume of air bubbles in the hydraulic oil	6.72×10^{-9} m^3
Air release time constant τ_r	5.88 s
Air re-solution time constant τ_s	11.35 s

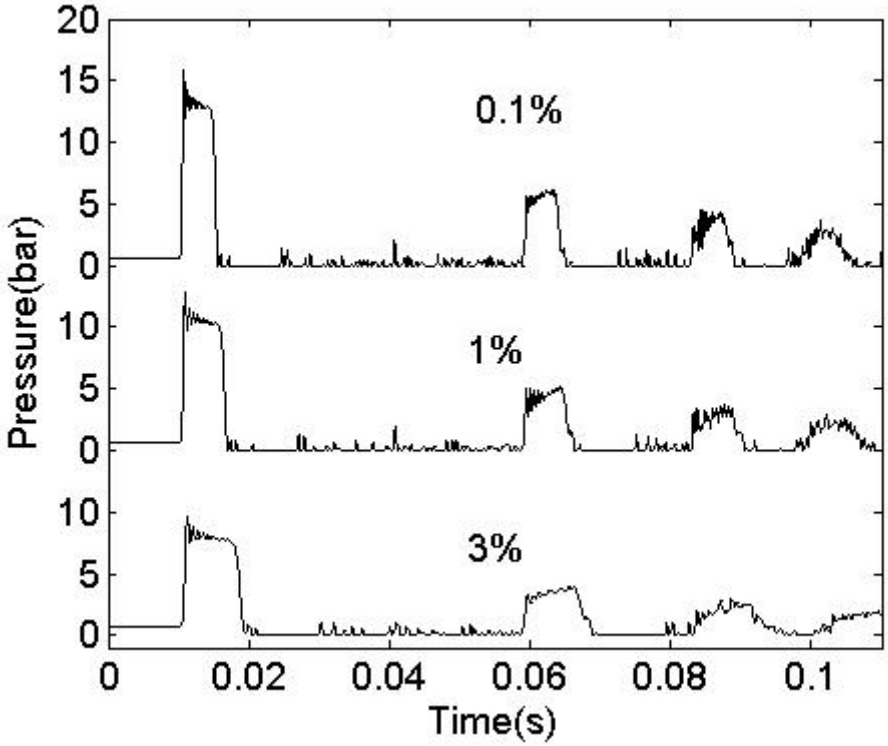

Fig. 1 Pressure pulsations with different initial volume of air bubbles

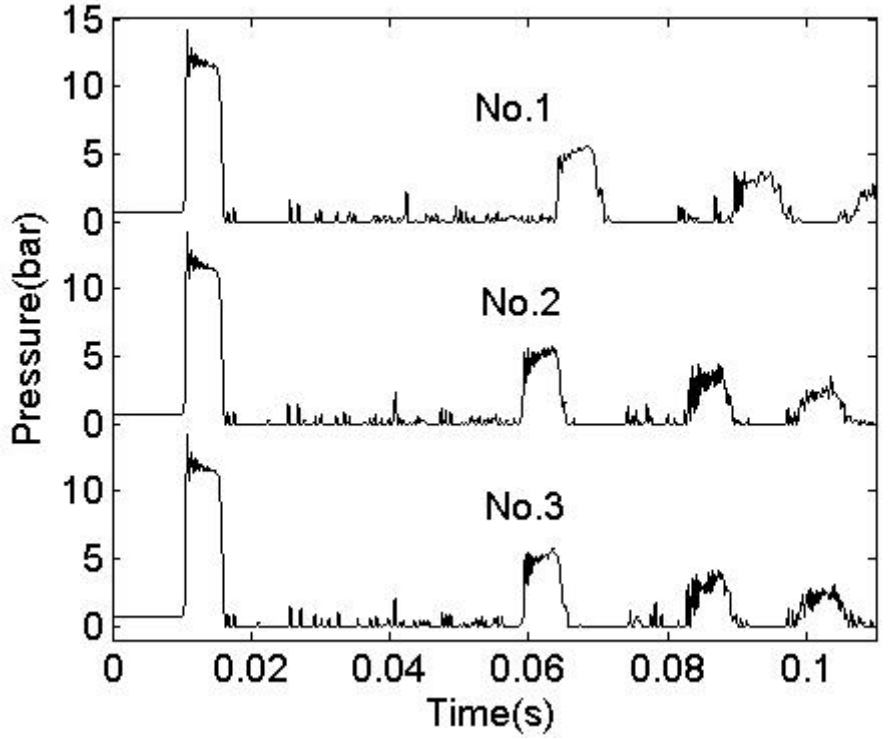

Fig. 2 Pressure transients for the parameters in Table 2

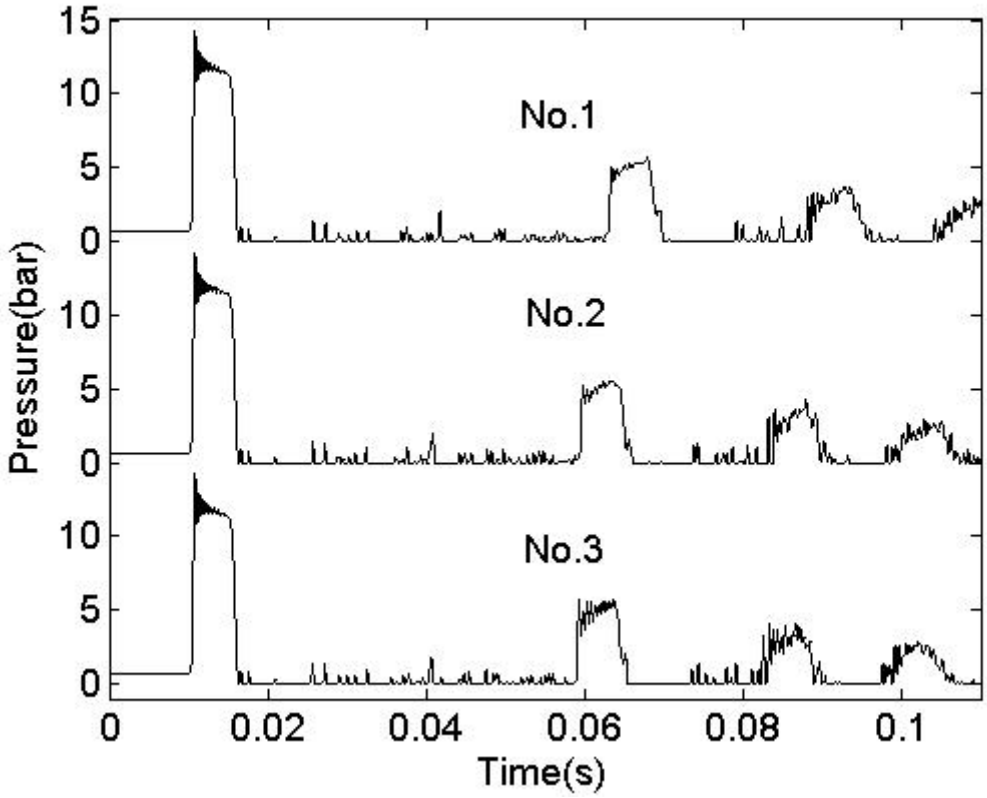

Fig. 3 Pressure transients for the parameters in Table 3

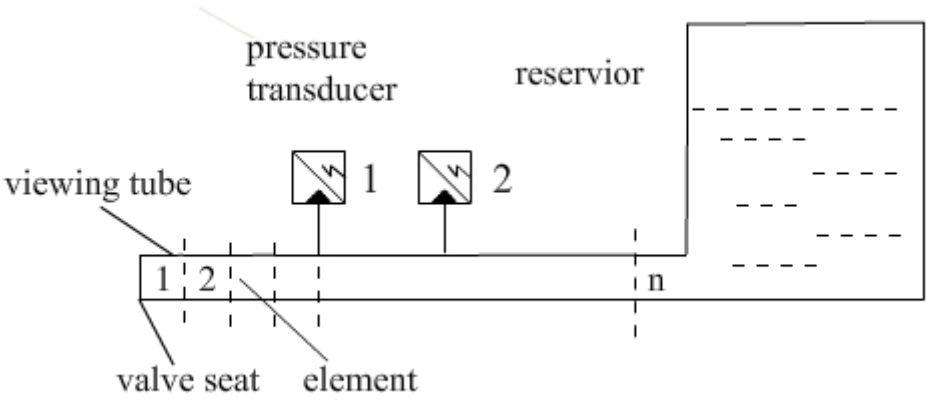

Fig. 4 Principle scheme for the experiments

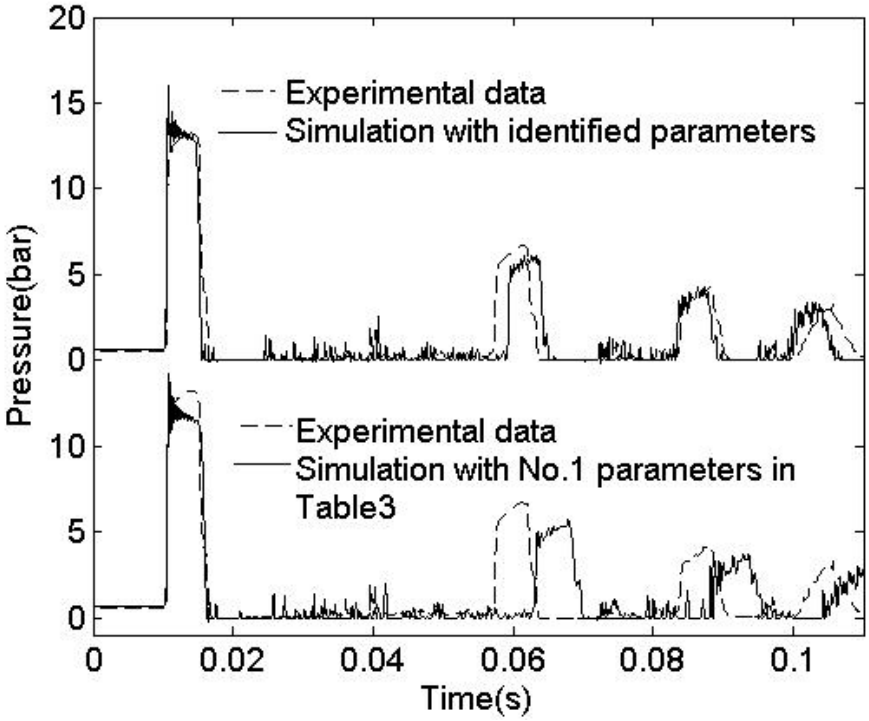

Fig.5 Comparison of simulation and experimental pressure transients at the first transducer

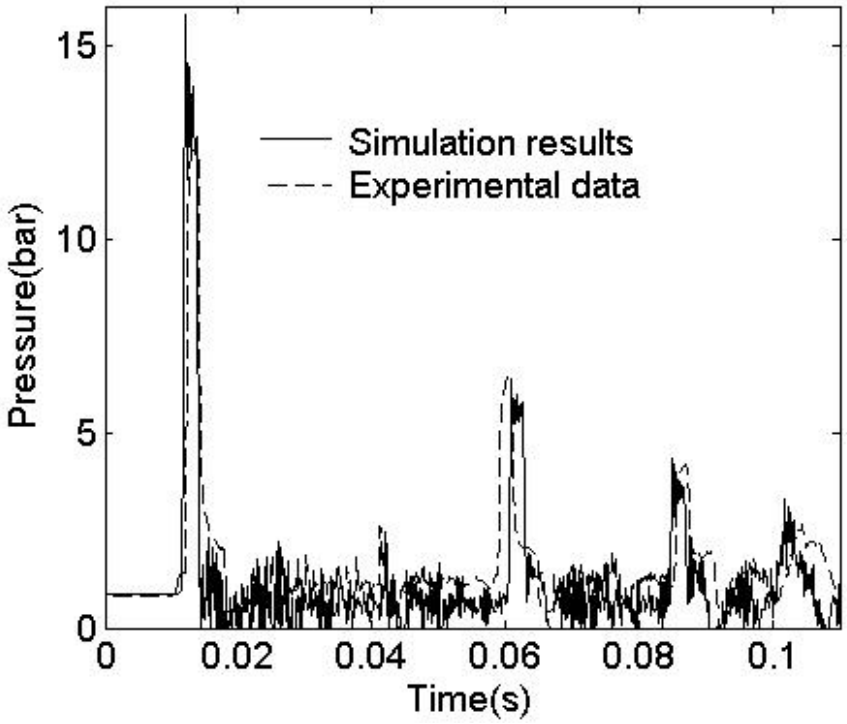

Fig.6 Comparison of simulation and experimental pressure transients at the position of the second transducer

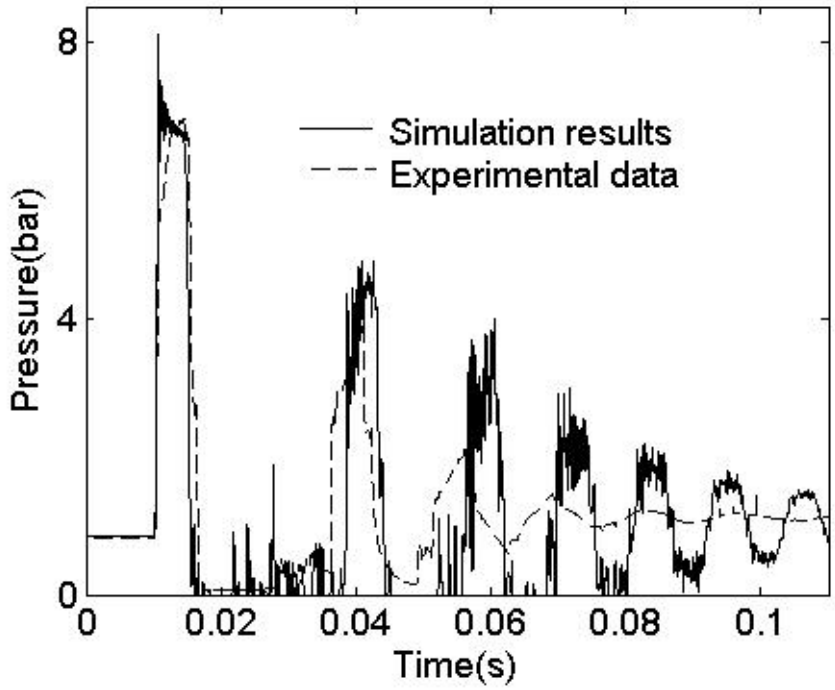

a) At the position of the first transducer

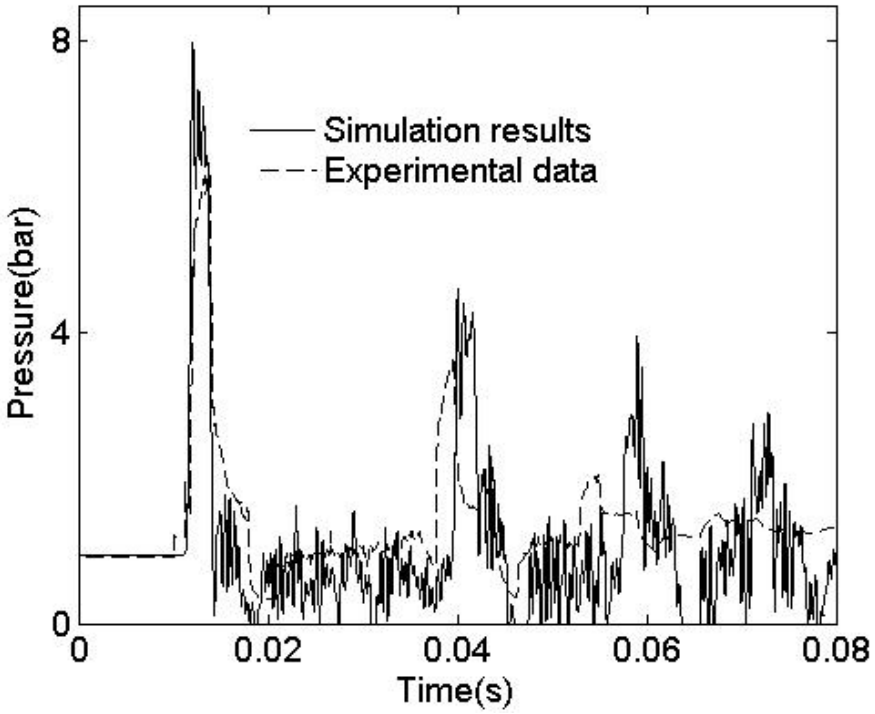

b) At the position of the second transducer

Fig.7 Comparison of simulation and experimental pressure transients at the lower flow rate

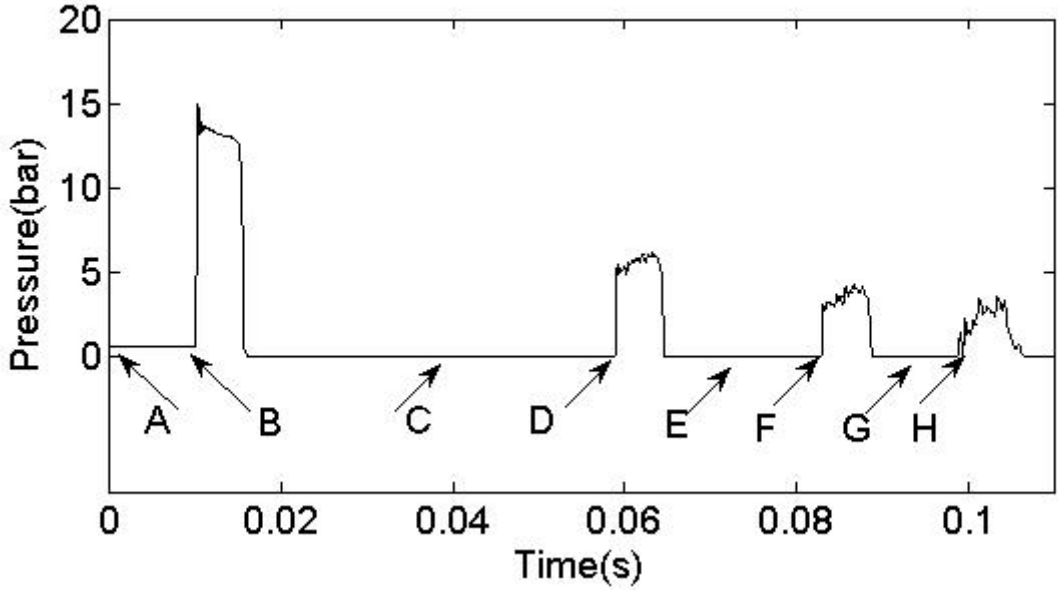

Fig. 8 Simulation result for the pressure transients in the first element

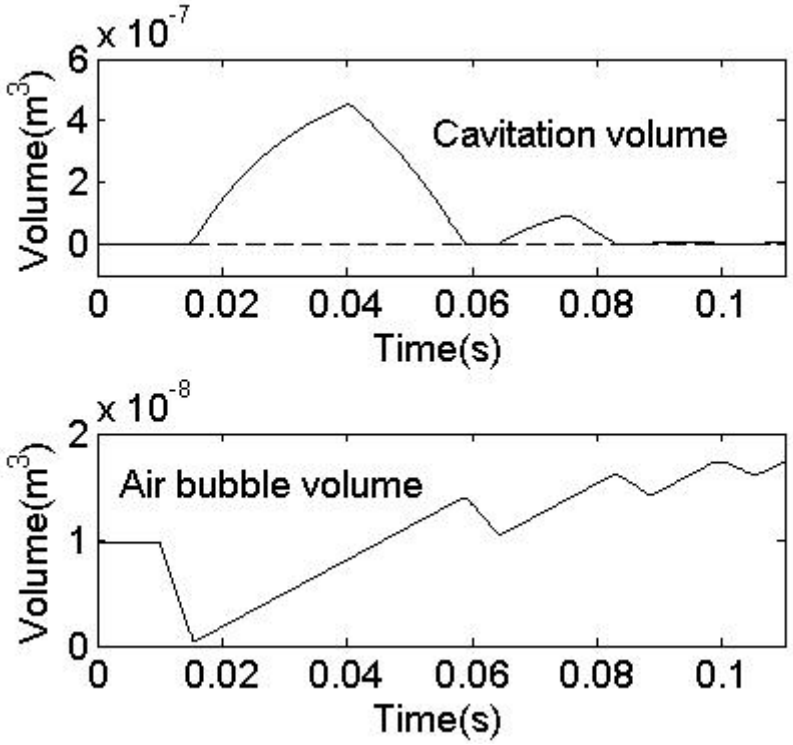

Fig.9 Predicted cavitation and air bubble volumes in the first element

(A) 0s

(B) 0.01s

(C) 0.038s

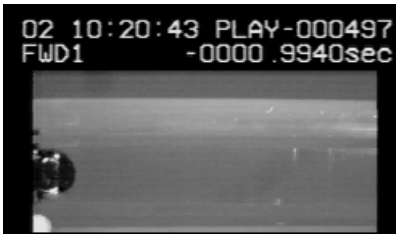

(D) 0.058s

(E) 0.074s

(F) 0.082s

(G) 0.096s

(H) 0.100s

Fig.10 Record of cavitation behaviour in the first element